Hindawi Publishing Corporation
Mathematical Problems in Engineering
Volume 2010, Article ID 517184, 13 pages
doi:10.1155/2010/517184

Research Article

Cooperative Control of Active Power Filters in Power Systems without Mutual Communication

Josef Tlustý,[1] Jiří Škramlík,[2] Jan Švec,[1] and Viktor Valouch[2]

[1] *Department of Power Engineering, Faculty of Electrical Engineering, Czech Technical University in Prague, Technická 2, 166 27 Prague 6, Czech Republic*
[2] *Department of Electric Machines, Drives, and Power Electronics, Institute of Thermomechanics, Academy of Sciences of the Czech Republic, Dolejškova 5, 182 02 Prague 8, Czech Republic*

Correspondence should be addressed to Jan Švec, jan.svec@fel.cvut.cz

Received 10 August 2010; Accepted 8 November 2010

Academic Editor: Ilmar Ferreira Santos

The procedure for calculating controller parameters of the APFs implemented into a multibus industrial power system for harmonic voltage mitigation is presented. The node-voltage-detection control strategy is applied and the basic controller parameters are found under the condition that the demanded THD factors at the buses where the APFs are placed will be obtained. A cooperative control of several APFs without mutual communication is proposed, simulated, and experimentally verified. By tuning the controller gains without considering the power circuit parameters, all APFs used tend to share harmonic load currents approximately equally regardless of the operation modes of the nonlinear loads in different parts of the power system.

1. Introduction

The performance and effectiveness of the active power filter (APF) depends on the point of its connection in the multibus power system [1–3].

The effectiveness of the bus voltage and branch current detection control strategies of the APFs used in multibus power systems was analyzed and compared in [4]. In [5] the *single APF-multiple harmonic optimization problem* was formulated in such a way that its solution yields optimum PI controller parameters of the APF for both the control methods.

In [6], an analytical solution of the *multiple APF-single harmonic problem* in the frequency domain was formulated. In the case study presented in [6] optimal compensator currents for individual harmonics in case of two APFs were calculated, interaction of the APFs analyzed and, finally, the best places for two APFs recommended.

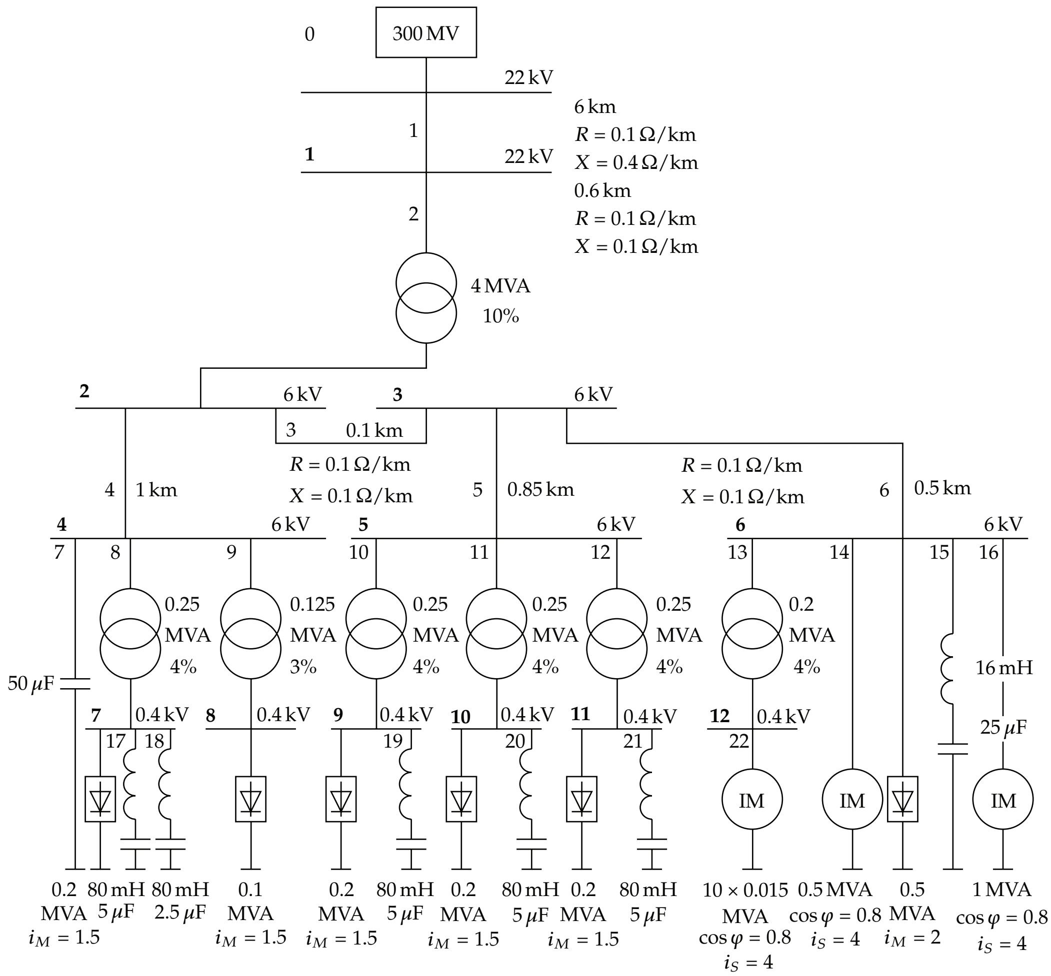

Figure 1: Multibus industrial power system.

In [7], an automatic gain adjustment of the APFs was introduced to make each APF damp out harmonic propagation throughout power distribution systems without considering the circuit parameters. The gain adjustment can reduce the APF compensating currents and losses.

In [8], a cooperative control of several APFs with the help of a communication system was proposed. Again, the APFs damp out harmonic propagation throughout power distribution systems. The APFs control gains are tuned by a computer on the basis of voltage total harmonic distortion (THD) at each APF place of installation. The control reduces the voltage THD at buses of the APFs installation and balances the compensating currents as well, irrespective of the power system conditions.

An instantaneous current control loop to ensure proper sharing of harmonic components of nonlinear loads among inverters in distributed generation systems is included in wireless controllers of these inverters [9]. Contrary to [7, 8], the output-voltage THD of distributed inverters are not directly included into the gain adjusting mechanism, although the algorithm helps to hold the voltage THD at a reasonable level.

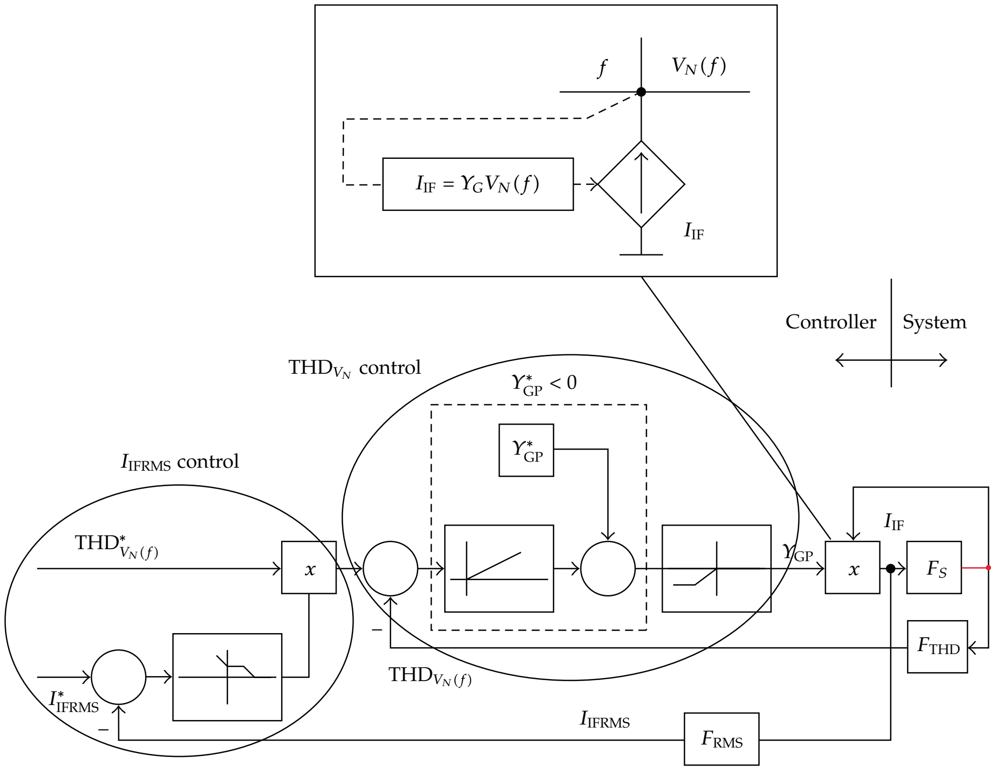

Figure 2: Self-tuning controller.

Also in [10], a harmonic droop scheme for sharing harmonic content of the load currents among distributed generation systems is proposed, being a part of a load-sharing controller that uses only low-bandwidth data communication signals among individual generation systems.

Finally, a distributed APF system for mitigating the harmonic distortion in power systems is proposed in [11]. A droop control strategy based on the VA rating of individual APFs ensures the distribution of the harmonic filtering workload in proportion to the rated capacity of every APF unit. The algorithm does not need the real-time communication among APF units. Again, the output-voltage THD of distributed inverters are not directly included into the gain-adjusting mechanism in [10, 11].

So, no wireless cooperative control strategy considering both the output-voltage THD of distributed inverters and the rated capacity of every APF has been reported till now.

Here, the *multiple APF-multiple harmonic problem* in case of applying the node-voltage-detection control strategy is formulated. A cooperative control without any communication of several APFs is proposed, simulated, and experimentally verified. The control aims, by tuning the controller gains without considering the power circuit parameters, at attaining the demanded THD of the voltages at the buses where the APFs are placed, provided that the VA ratings of individual APFs are not exceeded. If the load of an APF tends to be higher than its rated capacity, the algorithm tunes the APF controller gain further to hold the APF below its nominal rating. Additionally, the APF is prevented from a too low load as well by applying this procedure. Thus, all APFs used tend to share harmonic load currents approximately

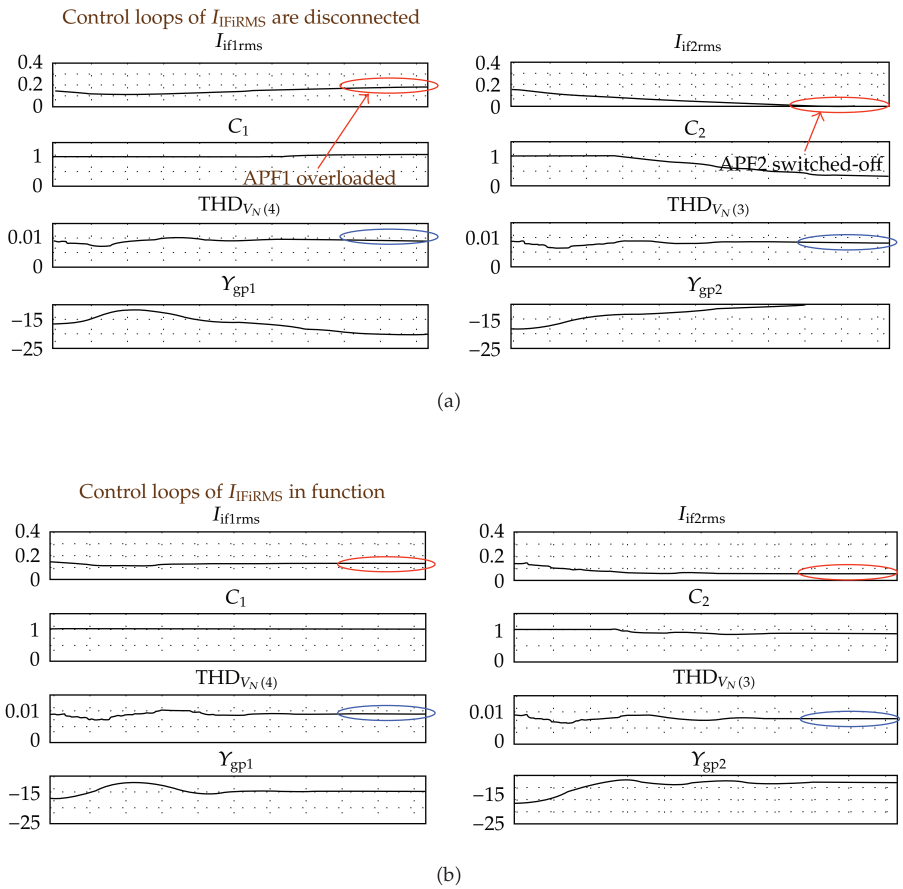

Figure 3: Transient processes following after increasing twice the current withdrawn by the rectifiers at the buses 7 and 8 and decreasing to zero the currents withdrawn by the rectifiers at the buses 9, 10, 11, and 6; (a) control loops of I_{IFiRMS} are disconnected, (b) control loops of I_{IFiRMS} in function.

equally regardless of the operation modes of the nonlinear loads in different parts of the power system.

2. Multibus Industrial Power System

An example of the multibus industrial power system shown in Figure 1 consists of overhead lines, cables, transformers, induction motors, rectifiers, and passive filters.

Some simplifications will be considered: the transformers and induction motors will be represented by inductances only, passive filters considered as ideal ones, without resistances, and ground capacitances of the lines and cables will be neglected as well. The rectifiers will be represented by ideal harmonic current sources I_{IL} with harmonic magnitudes determined by respective apparent powers, overload capacities, and by the so-called magnitude law. On the basis of the diagram of this system an equivalent circuit may be determined and the parameters of circuit elements calculated.

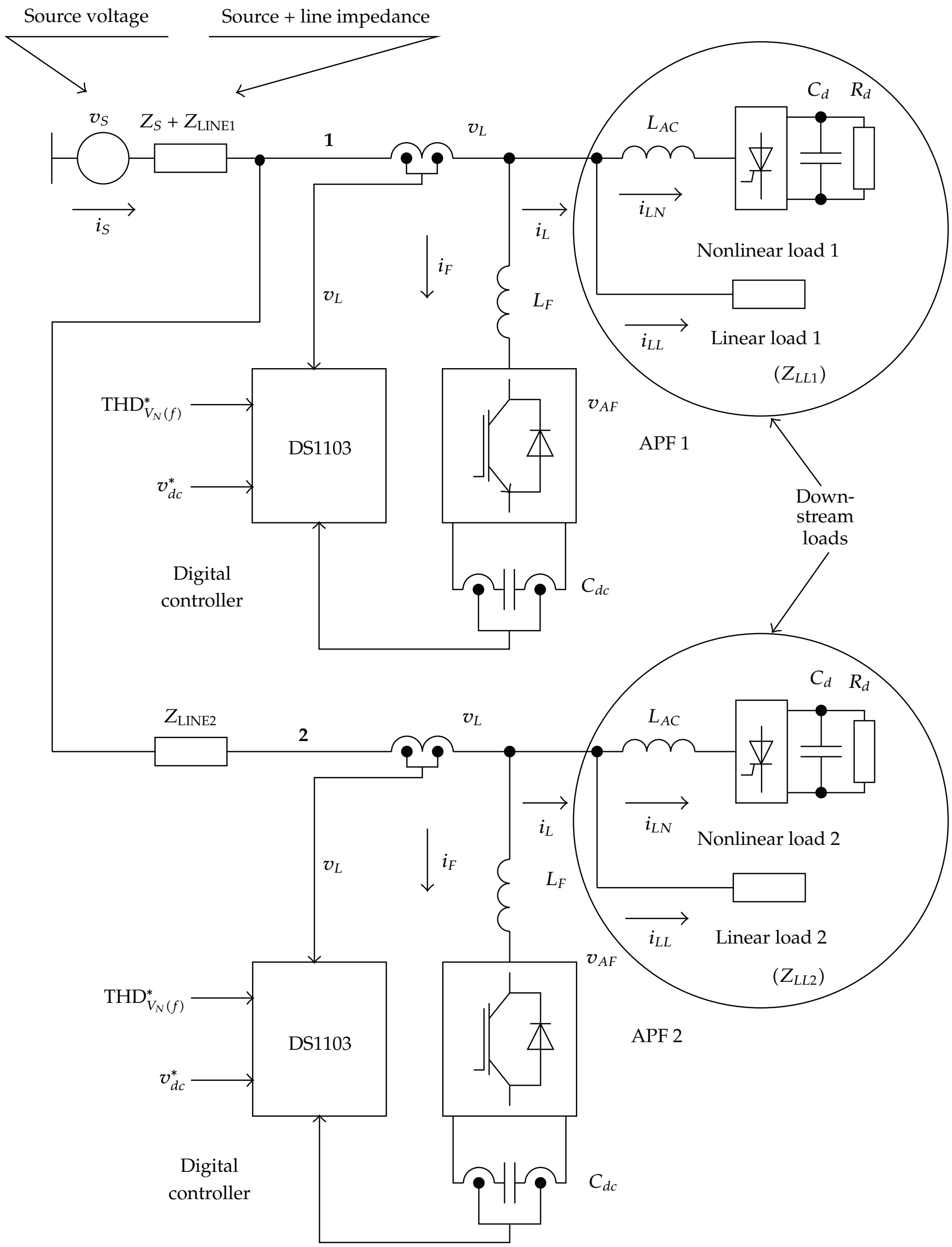

Figure 4: Experimental setup with two APFs working without communication.

The potential places for APFs are bus-bars with the voltage level of 6 kV, that is the bus-bars 2–6. APFs will be represented here by voltage-controlled current sources, that is by the vector I_{IF} of reference currents of the individual APFs. The agreement between the real and reference APF currents depends on an inner control strategy of the real APF that is

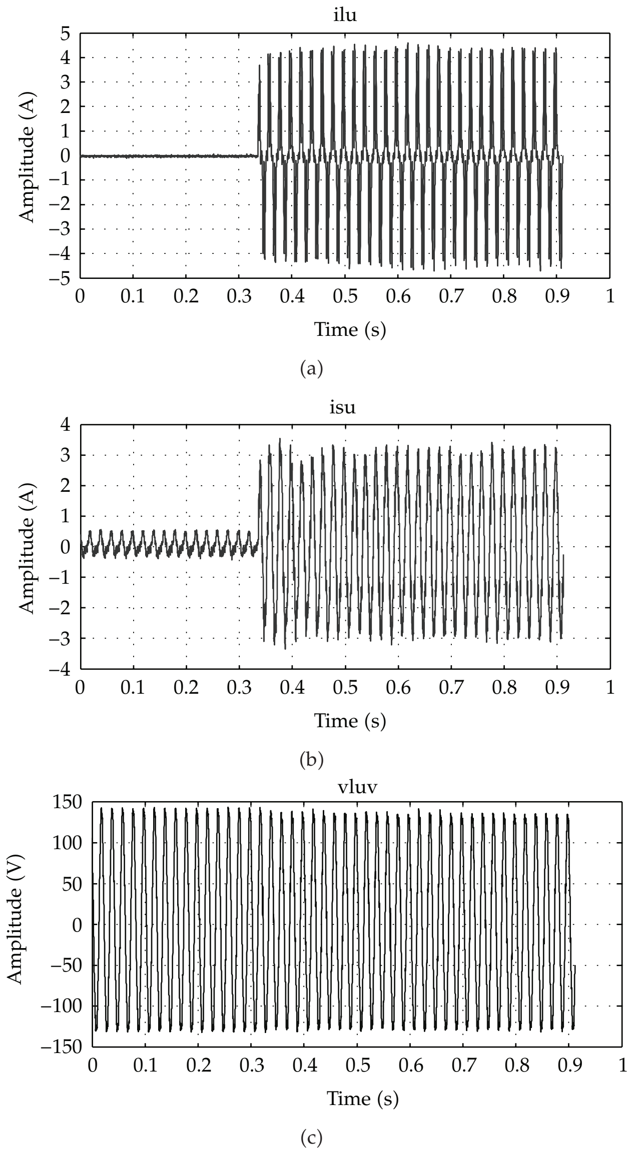

Figure 5: Waveforms of the load current (a), grid current in branch 1 (b), and line-to-line voltage (c) after switching load in this branch 1 on.

not analyzed here. Especially for dominant harmonic orders this agreement is reported to be quite well, though.

In the following analysis all quantities will be recalculated to the 6 kV level and expressed in the p.u. system with $S_B = 1\,\text{MVA}$ (the maximum power of the major rectifier, which is connected to the bus 6), $V_B = 6\,\text{kV}$, 50 Hz.

3. Control Strategies

The voltage and current detection feedback control strategies belong among control strategies very often used for parallel APFs applied in simple power distribution systems. We proposed

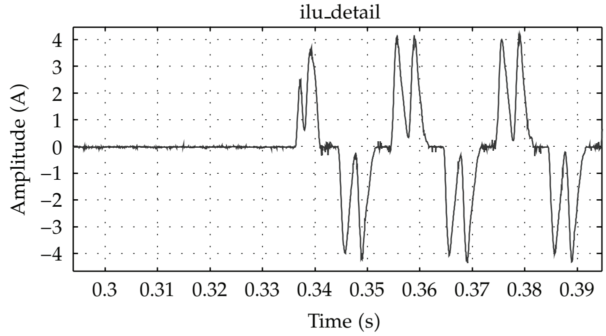

(a)

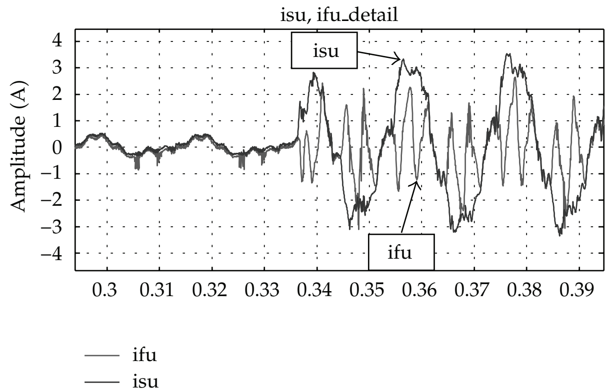

(b)

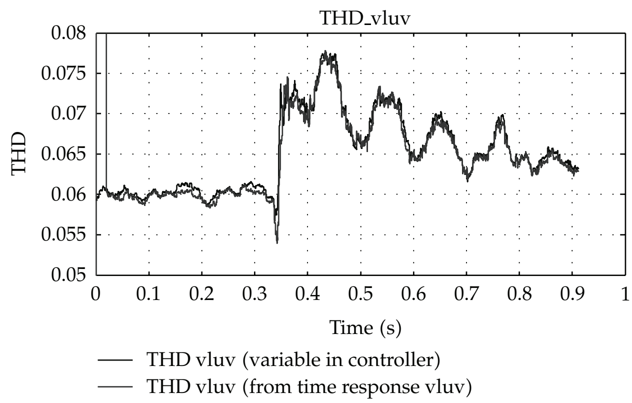

(c)

Figure 6: Details of the load current (a), grid and APF currents (b), and THD of line-to-line voltage (c) after switching load in this branch 1 on.

an application of these strategies in multibus industrial power systems with a few harmonic power sources [4, 5]. The effectiveness of the connection of the APF at a specific bus may be assessed by the degree of the voltage harmonic mitigation at selected buses and by the demanded value of the APF current I_{IFRMS}; but, the values of the controller gains should be

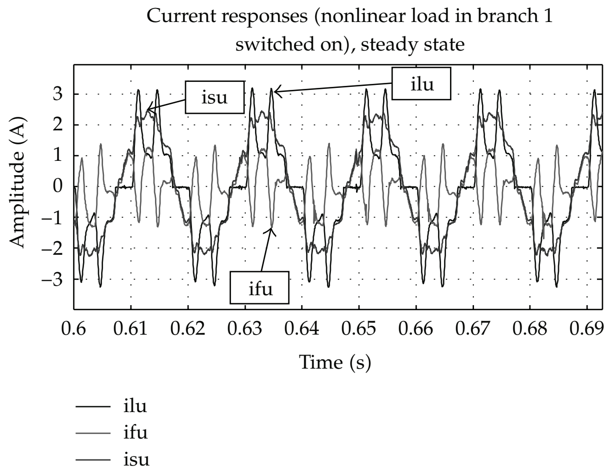

Figure 7: Waveforms of the load, APF, and grid current in the branch 1 in steady state.

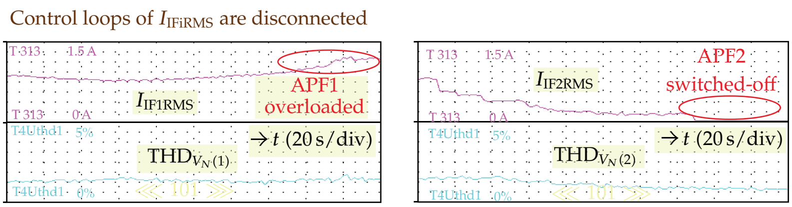

(a)

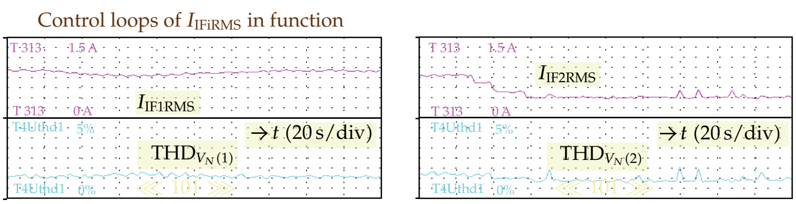

(b)

Figure 8: Transient processes following after: (1) increasing nonlinear load 1 by 50% and (2) disconnecting nonlinear load 2; (a) control loops of I_{IFiRMS} are disconnected, (b) control loops of I_{IFiRMS} in function.

taken into consideration as well, with regard to problems with stability of the whole control system.

We will analyze an application of the voltage detection feedback control strategy in multibus industrial power systems with a few harmonic power sources and several APFs.

Let the current vector I_{IF} of APFs be generated by using a feedback of the node voltage vector V_N

$$I_{\mathrm{IF}} = Y_G V_N, \tag{3.1}$$

where Y_G is the feedback gain matrix.

4. Multiple Harmonic Problem

For the *multiple APF-multiple harmonic problem* the objective function may be written

$$g_H = \sum_{h=2}^{H} \sum_{i=1}^{n-1} a_i^h \left| V_N^h(i) \right|^2, \tag{4.1}$$

where the weighting factor a_i $(0 \le a_i \le 1,\ i = 1, \ldots, n-1)$ reflects the different importance of the harmonic voltage mitigation at different nodes.

The formulae for the hth harmonic of the voltage $V_N^h(i)$ at the node i, which include the parameters of the controllers of APFs, should be formulated. The optimum values of the controller parameters may be determined by finding the minimum of g_H (4.1) for $V_N^h(i)$ declared.

Here, the objective function (4.1) will be used for solving the *multiple APF-multiple harmonic problem* in case of applying the node-voltage-detection control strategy. For finding optimum parameters of the controllers of the APFs, the relation for the hth harmonic of the voltage $V_N^h(i)$, determined in [5] for the single APF, must be reformulated to be valid for more than only one APF placed at the node f.

Because

$$V_N^h = V_{N0}^h + Z_{\mathrm{NIF}}^h I_{\mathrm{IF}}^h, \tag{4.2}$$

where Z_{NIF}^h is a transfer impedance matrix of the injected APF currents, V_{N0}^h is the node voltage vector without any compensation, and

$$I_{\mathrm{IF}}^h = Y_G^h V_N^h \tag{4.3}$$

determines the node-voltage-detection control strategy, the node voltage vector may be expressed by

$$V_N^h = -\left(Z_{\mathrm{NIF}}^h Y_G^h - E \right)^{-1} V_{N0}^h. \tag{4.4}$$

The elements of this voltage vector enter the objective function (4.1).

In the process of minimization of the objective function the optimum parameters Y_{Gi}, $i = 1, \ldots, m_F$ for the m_F controllers can be found.

But, in most of real cases the minimum value of the objective function, which is the power of the global value of THD of voltages (in p.u. system and over the whole number of bus-bars in question), is not necessary to reach. The attaining of predefined values of THDs of the voltages at the bus-bars where the APFs are placed seems to be a more practical aim. Then, the harmonic currents generated by the APFs may be remarkably lower than those needed in case of the mentioned global optimization obtained by the minimization of the objective function (4.1).

But, a question still remains whether THDs of voltages at the other bus-bars (where the APFs are not placed) will be sufficiently low to conform to our demands. Thus, comparing these THDs of voltages at remaining bus-bars of the industrial power system for different combinations of APFs places may be a key to find the best places for the APFs in this case.

For finding the parameters of the controllers for two APFs, which ensure that the predefined values of $\mathrm{THD}^*_{V_N(i)}$, $i = f1, f2$ at the bus-bars $f1$, $f2$ are attained, the objective function (4.1) should be modified as follows

$$g_H(f1, f2) = \sum_{i=f1,f2} \left[\sum_{h=2}^{H} a_i^h \left| V_N^h(i) \right|^2 - \left(\mathrm{THD}^*_{V_{N(i)}} \right)^2 \right]. \quad (4.5)$$

5. Self-Tuning Controller of APF

By using the strategy presented in the previous paragraph we can find a proper place and controller parameters, or at least to identify places unsuitable for the APF. The analysis assumes that the system parameters and harmonic current sources are known. Such an analysis may be done as the first step of the solution of the problem with some nominal system parameters and operating modes of harmonic current sources (mostly rectifiers).

But, the parameters in a real system are not precisely known and, especially, the harmonic spectra of the current sources are changing due to changes in a manufacturing process. Thus, a simple and efficient way to tune the controller parameters of the APF is very desirable.

We have two indicators to be checked, namely the current I_{IFRMS} that should not exceed its nominal value for the APF used and the real value of $\mathrm{THD}_{V_N(f)}$ that should not be much higher than its prescribed limit $\mathrm{THD}^*_{V_N(f)}$, because in such a case there is a real danger of an increase of $\mathrm{THD}_{V_N(i)}$ at the remaining bus-bars and of the global index THD_{V_N} all over the system too. On the other hand, an operation of the APF with $I_{\mathrm{IFRMS}} \leq I_{\mathrm{IFRMSnom}}$, if $\mathrm{THD}_{V_N(f)} \leq \mathrm{THD}^*_{V_N(f)}$, is not very economical either, and it is possible either to switch the APF off or to decrease $\mathrm{THD}^*_{V_N(f)}$ and, as a consequence, the values of $\mathrm{THD}_{V_N(i)}$ and THD_{V_N} as well.

Figure 2 shows the scheme of a self-tuning controller of the APF. The input variables are the reference $\mathrm{THD}^*_{V_N(f)}$ and I^*_{IFRMS}. The required value of $\mathrm{THD}^*_{V_N(f)}$ is compared with the real value $\mathrm{THD}_{V_N(f)}$, and the error enters a block where the gain Y_{GP} of the APF controller is determined.

A possible configuration is that the basic value Y^*_{GP} of the gain is modified by the output of the I-type controller with fairly low gain. Because the higher the negative value of the control error $-(\mathrm{THD}^*_{V_N(f)} - \mathrm{THD}_{V_N(f)})$ is, the higher the absolute values of the gain Y_{GP} and I_{IF} are; a limiter of the presented type should be used.

The real value I_{IFRMS} of the AFP current is compared with its required (nominal) value I^*_{IFRMS} and the error is proceeded in a nonlinear block, whose output (let us call it as constant C) modifies the reference value $\mathrm{THD}^*_{V_N(f)}$ of the voltage at the bus where the APF is placed. Thus, the reference $\mathrm{THD}^*_{V_N(f)}$ is modified in order that it may be obtained without exceeding the required (nominal) value I^*_{IFRMS} of the current generated by the APF.

If the error $I^*_{\mathrm{IFRMS}} - I_{\mathrm{IFRMS}}$ is positive up to some specific value, the reference $\mathrm{THD}^*_{V_N(f)}$ is not modified because the output of the nonlinear block has the value 1. But, for $(I^*_{\mathrm{IFRMS}} - I_{\mathrm{IFRMS}}) < 0$ the output of the block is going up quickly and increases the value of $\mathrm{THD}^*_{V_N(f)}$, which leads to a decrease of the APF current I_{IFRMS} and the error $I^*_{\mathrm{IFRMS}} - I_{\mathrm{IFRMS}}$ becomes lower. On the other hand, a big positive error $I^*_{\mathrm{IFRMS}} - I_{\mathrm{IFRMS}}$ can result in that the lower value $\mathrm{THD}^*_{V_N(f)}$ is required and achieved. Another option is that this big positive-error value may be the impetus for switching the APF off.

It is evident that the control loop of the APF current I_{IFRMS} is superior to the control loop of $\mathrm{THD}_{V_N(f)}$ of the voltage where the APF is placed.

6. Simulation

Let us verify some key results, conclusions, and also the function of the controller proposed in the previous chapter by the simulation in the time domain.

The industrial power system shown in Figure 1 was simulated by using Matlab-Simulink.

The APFs were placed at the bus-bars 3 and 4 and equipped with the controller presented in Figure 2. Time and all variables are expressed in p.u. related to the nominal frequency 50 Hz, the voltage 6 kV, and to the maximum power of the biggest rectifier connected at the bus-bar 6.

The reference variables were set like this: $\mathrm{THD}^*_{V_N(j)} = 0.009$; $I^*_{\mathrm{IFRMS}} = 0.15$ p.u.; $Y^*_{\mathrm{GP}} = -0.5$ p.u. for both the APFs.

Figure 3(a) shows transient processes following after increasing twice the currents withdrawn by the rectifiers at the buses 7 and 8 and decreasing to zero the currents withdrawn by the rectifiers at the buses 9, 10, 11, and 6. The responses of the following variables are shown from up to bottom: I_{IFiRMS}, constant C_i at the output of the nonlinear block modifying the reference value $\mathrm{THD}^*_{V_N(j)}$, $\mathrm{THD}_{V_N(j)}$, $Y_{\mathrm{GP}i}$, $i = 1, 2$ (number of the APF), and $j = 4, 3$ (the place of the APF). The control loops of I_{IFiRMS} are disconnected now, so changes of the constants C_i do not affect $\mathrm{THD}^*_{V_N(j)} = 0.009$.

We can see that the APF2 placed at the bus 3, which lies upstream the buses 9–12, goes out of the operation $I_{\mathrm{IF2RMS}} = Y_{\mathrm{GP2}} = 0$, while the current $I_{\mathrm{IF1RMS}} = 0.181$ p.u. of the APF 1 becomes higher than its nominal value. The reason is that the value of $\mathrm{THD}_{V_N(3)} = 0.0081$ is lower than its reference $\mathrm{THD}^*_{V_N(3)} = 0.009$ in the final steady state.

Figure 3(b) shows the similar transient processes, but the I_{IFiRMS} control loops of the APFs are in function now. The result is that both the APFs remain in operation with $I_{\mathrm{IF1RMS}} = 0.133$ p.u. and $I_{\mathrm{IF2RMS}} = 0.060$ p.u., that is under the nominal value $I^*_{\mathrm{IFRMS}} = 0.15$ p.u., and with $\mathrm{THD}_{V_N(4)} = 0.0090$ and $\mathrm{THD}_{V_N(3)} = 0.0078$.

7. Experimental Verification

The function of the proposed control strategy of several APFs in the power system without their mutual communication has been experimentally verified. Figure 4 shows an experimental setup that consists of two pairs of a nonlinear and linear load.

These loads are connected to the source voltage via different impedances Z_{LINE1} and Z_{LINE2} that represent impedances of the lines, cables, and transformers of a real power system. Two APFs are placed in parallel with these load pairs. The control algorithm presented in Figure 2 is implemented into both dSPACE DS1103 control systems of APFs.

Figures 5–7 demonstrate the function of the control loop of $\mathrm{THD}_{V_N(1)}$ of the APF1. Figure 8 shows how the superior current control loops prevent overloading of the APFs.

Figure 5 shows the waveforms of the load current (a), grid current in the branch 1 (b), and line-to-line voltage (c) after switching the load in this branch 1 (Figure 4) on.

Figure 6 presents the respective details of the load current (a), grid and APF1 currents (b), and THD of line-to-line voltage (c) after switching the load in the branch 1 on. The current $i_{\mathrm{su}} = i_{\mathrm{fu}}$ in Figure 6(b) before the load in the branch 1 is switched on is generated by the APF1 to hold $\mathrm{THD}_{V_N(1)}$ equal to $\mathrm{THD}^*_{V_N(1)} = 0.06$, because the full load in the branch 2 is applied. In Figure 6(c) two waveforms are shown: the first one is the signal $\mathrm{THD}_{V_N(1)}$ in the APF digital controller, the second one is a result of analysis of the captured voltage v_{luv} from Figure 5(c) made a posteriori the experiment. Both the curves feature a very good agreement.

Figure 7 shows the waveforms of the load, APF, and grid current in the branch 1 in steady state. It is evident that load current harmonics are effectively mitigated by the respective APF1.

Figure 8 shows transient processes following after: (1) increasing nonlinear load 1 by 50% and (2) disconnecting nonlinear load 2.

It is evident that the APF 1 is overloaded and the APF 2 is switched-off if the APF control loops of I_{IFiRMS}, $i = 1, 2$ are disconnected and only the control loops of $\mathrm{THD}_{V_N(1)}$, $\mathrm{THD}_{V_N(2)}$ are in function. Contrary to that, both the APFs remain in operation if the superior control loops of I_{IFiRMS}, $i = 1, 2$ of both the APFs are in function. The values of $I^*_{\mathrm{IF1RMS}} = I^*_{\mathrm{IF2RMS}}$ were set at 1 A and $\mathrm{THD}_{V_N(1)} = \mathrm{THD}_{V_N(2)} = 1.5\%$. The experimental results are in a good agreement with those obtained by simulation, Figure 3.

8. Conclusion

The procedure for calculating controller parameters of the APFs implemented into the multibus power system has been presented. The node-voltage-detection control strategy was applied and the controller parameters were found by solving the modified *multiple APF-multiple harmonic problem* under the condition that demanded THD factors at the buses where the APFs are placed will be obtained.

A cooperative control of several APFs without any communication has been proposed and simulated as well. By tuning the controller gains without considering the power circuit parameters, all APFs used tend to share harmonic load currents approximately equally regardless of the operation modes of the nonlinear loads in different parts of the power system.

Acknowledgments

The financial support of the Grant Agency of the Academy of Sciences of the Czech Republic (project no. IAA200760703), Institutional Research Plan Z20570509 of the Institute of Thermomechanics of the ASCR, v.v.i., and of the Ministry of Education, Youth, and Sports (Research Plan MSM 6840770017 of the Czech Technical University) are highly acknowledged.

References

[1] X. Dai and R. Gretsch, "Optimal compensator currents for the reduction of the harmonic distortion in networks. Part 1: analytic solution," *European Transactions on Electrical Power Engineering*, vol. 4, no. 4, pp. 301–307, 1994.

[2] K. Mikolajuk, "The problem of harmonic compensators location," *European Transactions on Electrical Power*, vol. 6, no. 6, pp. 397–400, 1996.

[3] L. T. Morán, J. J. Mahomar, and J. R. Dixon, "Careful connection," *IEEE Industry Applications Magazine*, vol. 10, no. 2, pp. 43–50, 2004.

[4] J. Tlustý, V. Valouch, P. Santarius, and J. Škramlík, "Optimal control of shunt active power filters in multibus industrial power systems for harmonic voltage mitigation," in *Proceedings of the International Conference on Electrimacs*, Hammamet, Tunisia, April 2005.

[5] J. Tlustý and V. Valouch, "Optimum controller gains of active power filters for harmonic voltage mitigation in multibus industrial power systems," in *Proceedings of the International Conference on Electrical Engineering (ICEE '05)*, Kunming, China, July 2005.

[6] W. Gawlik, "Optimal placement and mutual influence of active filters," in *Proceedings of the 17th International Conference on Electricity Distribution (CIRED '03)*, pp. 1–5, Barcelona, Spain, May 2003.

[7] P. Jintakosonwit, H. Akagi, and H. Fujita, "Performance of automatic gain adjustment in shunt active filters for harmonic damping throughout power distribution systems," in *Proceedings of the 32nd IEEE Annual Power Electronics Specialists Conference*, pp. 1389–1395, Vancouver, Canada, June 2001.

[8] P. Jintakosonwit, H. Fujita, H. Akagi, and S. Ogasawara, "Implementation and performance of cooperative control of shunt active filters for harmonic damping throughout a power distribution system," *IEEE Transactions on Industry Applications*, vol. 39, no. 2, pp. 556–564, 2003.

[9] J. M. Guerrero, L. G. de Vicuna, J. Matas, M. Castilla, and J. Miret, "A wireless controller to enhance dynamic performance of parallel inverters in distributed generation systems," *IEEE Transactions on Power Electronics*, vol. 19, no. 5, pp. 1205–1213, 2004.

[10] M. N. Marwali, J. W. Jung, and A. Keyhani, "Control of distributed generation systems. Part II: load sharing control," *IEEE Transactions on Power Electronics*, vol. 19, no. 6, pp. 1551–1561, 2004.

[11] P. T. Cheng and T. L. Lee, "Distributed active filter systems (DAFSs): a new approach to power system harmonics," *IEEE Transactions on Industry Applications*, vol. 42, no. 5, pp. 1301–1309, 2006.